Arabidopsis SMG7 protein is required for exit from meiosis

Nina Riehs[1,*], Svetlana Akimcheva[1,*], Jasna Puizina[1,‡], Petra Bulankova[1], Rachel A. Idol[2,§], Jiri Siroky[3], Alexander Schleiffer[4], Dieter Schweizer[1], Dorothy E. Shippen[2] and Karel Riha[1,¶]

[1]Gregor Mendel Institute of Molecular Plant Biology, Austrian Academy of Sciences, Dr Bohr-Gasse 3, 1030 Vienna, Austria
[2]Department of Biochemistry and Biophysics, Texas A&M University, College Station, TX 77843-2128, USA
[3]Institute of Biophysics, Czech Academy of Sciences, 612 65 Brno, Czech Republic
[4]Research Institute of Molecular Pathology, 1030 Vienna, Austria

*These authors contributed equally to this work
‡Present address: Department of Biology, University of Split, Teslina 12, Croatia
§Present address: Department of Internal Medicine, Division of Hematology, Division of Laboratory Medicine, Washington University School of Medicine, St Louis, MO 63110, USA
¶Author for correspondence (e-mail: karel.riha@gmi.oeaw.ac.at)

Accepted 9 April 2008
Journal of Cell Science 121, 2208-2216 Published by The Company of Biologists 2008
doi:10.1242/jcs.027862

Summary

Meiosis consists of two nuclear divisions that are separated by a short interkinesis. Here we show that the SMG7 protein, which plays an evolutionarily conserved role in nonsense-mediated RNA decay (NMD) in animals and yeast, is essential for the progression from anaphase to telophase in the second meiotic division in *Arabidopsis*. *Arabidopsis SMG7* is an essential gene, the disruption of which causes embryonic lethality. Plants carrying a hypomorphic *smg7* mutation exhibit an elevated level of transcripts containing premature stop codons. This suggests that the role of SMG7 in NMD is conserved in plants. Furthermore, hypomorphic *smg7* alleles render mutant plants sterile by causing an unusual cell-cycle arrest in anaphase II that is characterized by delayed chromosome decondensation and aberrant rearrangement of the meiotic spindle. The *smg7* phenotype was mimicked by exposing meiocytes to the proteasome inhibitor MG115. Together, these data indicate that SMG7 counteracts cyclin-dependent kinase (CDK) activity at the end of meiosis, and reveal a novel link between SMG7 and regulation of the meiotic cell cycle.

Supplementary material available online at
http://jcs.biologists.org/cgi/content/full/121/13/2208/DC1

Key words: Anaphase, APC, CDK, Mitosis

Introduction

Entry into mitosis is characterized by increased activity of mitotic kinases, which peaks at metaphase and rapidly declines during anaphase. The transition from metaphase to anaphase is triggered by inactivation of the spindle checkpoint, which is a surveillance mechanism that prevents precocious separation of sister chromatids before all chromosomes have properly attached to the mitotic spindle (Taylor et al., 2004). Following chromosome congression and biorientation, the inhibitory signal of the spindle checkpoint is shut off and an E3 ubiquitin ligase called the anaphase-promoting complex (APC, also known as ANAPC) is free to target mitotic cyclins and securin for proteolytic degradation (Peters, 2006). Securin destruction leads to the activation of separase, the protease that cleaves the cohesin complex and thus triggers separation of sister chromatids and anaphase entry (Petronczki et al., 2003; Watanabe, 2004). Degradation of mitotic cyclins by the APC promotes cell-cycle progression by decreasing the activity of cyclin-dependent kinases (CDKs). A switch from high to low CDK activity during anaphase is essential for coordinating chromosome movement and spindle rearrangements as well as for processes associated with cytokinesis and exit from mitosis (de Gramont and Cohen-Fix, 2005). Thus, the activation of the APC couples chromosome segregation with the processes that are required for the M-G1 transition and cytokinesis. In budding yeast, late mitotic events are further coordinated by activation of the FEAR and MEN networks that control the release of Cdc14 phosphatase, which is a major antagonist of mitotic CDKs (Stegmeier and Amon, 2004; Queralt et al., 2006). Analogous mechanisms that govern the transition from high to low CDK activity and mitotic exit in higher eukaryotes are not well characterized.

The key mechanisms controlling mitotic progression are also effective in meiosis, although extensive modifications have evolved, particularly during the first reductional division, to allow the formation of four haploid nuclei after two successive rounds of chromosome separation. Whereas meiosis I is characterized by several unique processes, such as chiasmata formation, mono-orientation of sister kinetochores and protection of centromeric cohesion, the second meiotic division resembles mitosis (Page and Hawley, 2003; Petronczki et al., 2003; Marston and Amon, 2004; Watanabe, 2004). Furthermore, whereas CDK activity is only partially destroyed at the end of meiosis I, preventing entry into S phase and chromosome reduplication (Iwabuchi et al., 2000; Izawa et al., 2005; Irniger, 2006), complete CDK inactivation must occur at the end of the second meiotic division to allow the transition to a subsequent G1 phase. Studies in frogs and fission yeast indicate that a high level of CDK activity is retained in meiotic interkinesis by reduced proteolysis as well as by increased synthesis of meiotic cyclins (Gross et al., 2000; Hochegger et al., 2001; Borgne et al., 2002; Izawa et al., 2005). However, mechanisms leading to a differential regulation of CDK activity after the first and second meiotic divisions are still only poorly understood.

In this study, we characterized a novel *Arabidopsis thaliana* gene (*SMG7*) that is crucial for completion of the meiotic cell cycle. The gene encodes a protein that possesses an evolutionarily conserved EST1 domain and exhibits strong homology to human SMG6 (EST1A) and SMG7 (EST1C) proteins, which are implicated in

nonsense-mediated RNA decay (NMD) and in telomere metabolism (Reichenbach et al., 2003; Snow et al., 2003; Unterholzner and Izaurralde, 2004; Fukuhara et al., 2005). We found that partial abrogation of *Arabidopsis* SMG7 function by hypomorphic mutations leads to complete sterility caused by a meiotic arrest in anaphase II. The cell-cycle arrest is characterized by a failure to decondense chromosomes and to reorganize the meiotic spindle. We further show that SMG7 deficiency affects NMD and leads to severe defects in vegetative growth. These data indicate that *Arabidopsis* SMG7 is fundamentally involved in several cellular processes.

Results

Identification of *Arabidopsis* SMG7 (EST1)-like proteins

The founding member of the EST1 family, the budding yeast Est1p (ever shorter telomere 1), was identified in a screen for genes that are essential for telomere replication (Lundblad and Szostak, 1989). Est1p binds the RNA subunit of telomerase and facilitates its recruitment to chromosome termini (Lundblad, 2003). Putative Est1p homologs have been found in other eukaryotic organisms, including mammals (Beernink et al., 2003; Chiu et al., 2003; Reichenbach et al., 2003; Snow et al., 2003). Homology between EST1 proteins has been described to be restricted to the ~250 amino acid N-terminal region that contains tetratricopeptide repeat (TPR) motifs, which we call here the EST1-TPR domain (supplementary material Fig. S1A). The genes encoding putative EST1 orthologs from *Arabidopsis* were identified in a position-specific iterated (PSI)–BLAST search (Altschul and Koonin, 1998). Using amino acids 100-300 of the *Kluyveromyces lactis* Est1 (AAG49579) as the query against the non-redundant (nr) database, the first iteration of PSI-BLAST identified *Saccharomyces cerevisiae* Est1p (ScEst1p; NP_013334), ScEbs1p (NP_010492) and *Schizosaccharomyces pombe* Est1p (SpEst1p; CAA21171). All three were added to the *K. lactis* sequence to create a position-specific scoring matrix (PSSM), which was then used to search the nr database. In the second iteration, the human protein SMG6 (hSMG6; BAA34452) and an *Arabidopsis* protein (AAF98429) were identified. The *Arabidopsis* protein was used as a query in a BLAST search against the *Arabidopsis* database. This search identified a protein that was 28% identical over the first ~550 amino acids to the query sequence (NP_197441). Iterative NCBI (National Center for Biotechnology Information) PSI-BLAST searches extend the homologous region to ~300 amino acids beyond the conserved EST1-TPR domain, referred to as EST1-CD (supplementary material Fig. S1B and A.S., unpublished data). Both *Arabidopsis* proteins exhibit strongest homology to human SMG7 and SMG6 (E-values <1e-20 in an NCBI blastp search within the NCBI non-redundant database). Because of a similar domain topology to human SMG7, we have called them SMG7 (AtSMG7; At5g19400) and SMG7-like (AtSMG7-like, AtSMG7L; At1g28260) (supplementary material Fig. S1B).

The sequence of the *Arabidopsis* SMG7L and SMG7 proteins was further confirmed by obtaining cDNAs of both mRNAs using reverse transcriptase (RT)-PCR and primers directed to the predicted start and stop codons. The sequences of the *SMG7L* cDNA products matched the corresponding full-length mRNAs in GenBank (NM_102591) derived from the gene At1g28260. However, sequence analysis of the *SMG7* cDNA obtained by RT-PCR and by 5′- and 3′-RACE (deposited in GenBank under accession number EU126544) revealed an alternative acceptor site within the seventh intron of the published *Arabidopsis SMG7* mRNA (NM_121945). The alternative splicing site is located downstream of the termination codon and does not change the amino acid sequence of the SMG7 protein. The presence of the two SMG7 paralogs in Arabidopsis appears to be specific to dicot plants because genes orthologous for both *SMG7* and *SMG7L* can be found in fully sequenced genomes of *Medicago sativa*, *Vitis vinifera* and *Populus trichocarpa*, but genomes of rice and the moss *Physcomitrella patens* contain only the *SMG7* ortholog (supplementary material Fig. S1C).

Arabidopsis SMG7 mutants exhibit growth defects and infertility

Biochemical and functional analyses of SMG7 in human cell lines suggest its involvement in NMD (Unterholzner and Izaurralde, 2004; Fukuhara et al., 2005). However, consequences of SMG7 dysfunction at the organismal level have not yet been reported. To examine the function of SMG7 in plants, we identified *Arabidopsis* mutants harboring T-DNA insertions in the *SMG7* and *SMG7L* genes (Fig. 1A and data not shown). Analysis of two independent *smg7l* T-DNA-insertion mutants did not yield any obvious phenotype related to plant growth and development or telomere function and maintenance (R.A.I. and D.E.S., unpublished data). Therefore, we focused our study on the *SMG7* gene.

Northern blot analysis showed that the *SMG7* gene is expressed in all examined plant tissues (Fig. 1B). We obtained three T-DNA-insertion mutants of *SMG7*: *smg7-1*, *smg7-3* and *smg7-5* (Fig. 1A). No plants homozygous for the *smg7*-5 mutation were obtained from 63 plants segregating from heterozygous parents. Siliques of the heterozygous plants contained a portion of aborted seeds (Fig. 1D) and the ratio of $SMG7^{+/-}$ to $SMG7^{+/+}$ plants was 2:1 (χ^2=1.78), indicating that the *smg7-5* allele is embryonic lethal.

By contrast, plants bearing the *smg7-1* and *smg7-3* mutations were viable, albeit that homozygous mutant plants exhibited severe growth retardation. The *smg7-1* mutants that were germinated directly in soil formed miniature plants with only a few true leaves. Such plants usually succumbed to massive necrosis within 4 weeks of germination (Fig. 1E). The *smg7-3* mutants developed a less-severe vegetative-growth phenotype, which was characterized by deformed rosette leaves and an enlarged shoot apical meristem (Fig. 1F). The plants grew very slowly, and rosette leaves developed necrotic spots and only rarely produced inflorescence bolts. Northern blot hybridization showed that expression of the *smg7-1* and *smg7-3* alleles produces truncated transcripts that can yield SMG7 N-terminal peptides consisting of 356 and 677 amino acids, respectively, which span the entire EST1-TPR domain (Fig. 1C and supplementary material Fig. S2). The less-severe phenotype compared with the *smg7-5* allele together with the northern blot hybridization data indicates that partially functional peptides are synthesized in these plants.

Interestingly, the defects in vegetative growth could be suppressed, to a large extent, by growing *smg7-1* and *smg7-3* seedlings on agar plates. When such in-vitro-cultivated seedlings were transferred to soil 3 weeks after germination, *smg7* mutants reached maturity and developed multiple short inflorescence bolts that gave plants a bushy appearance (Fig. 1G). The inflorescent bolts were weaker than in wild-type plants, with short internodes and sterile flowers (Fig. 1H). Complete sterility was an invariant feature of both *smg7-1* and *smg7-3* mutants. Normal growth and fertility could be restored by complementing the *smg7-1* mutation with constructs expressing *SMG7* cDNA from actin or 35S promoters (data not shown). These data demonstrate that the observed phenotypes are specifically linked to the loss of SMG7 function. The developmental defects do not appear to be a

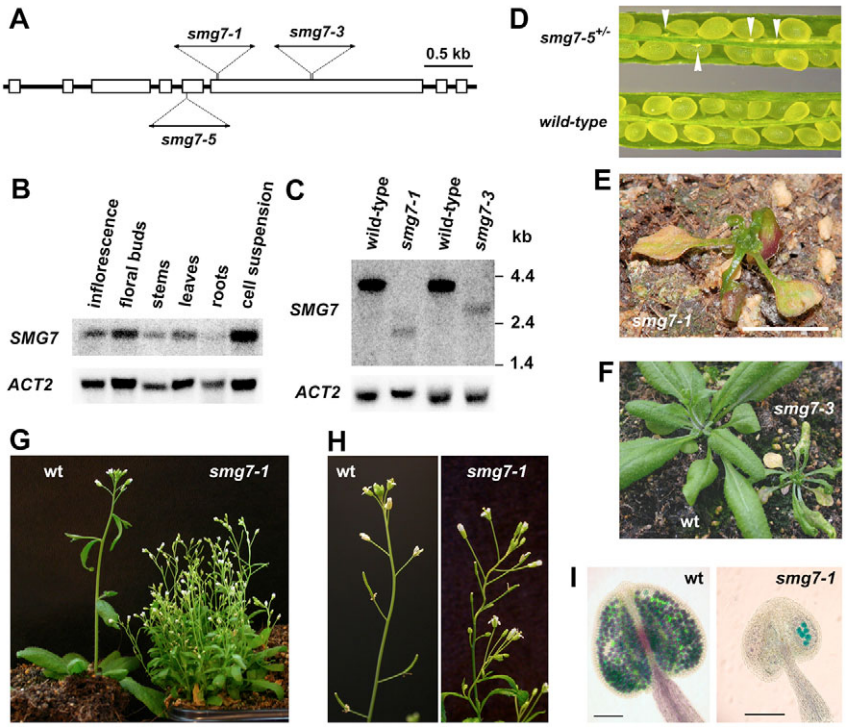

Fig. 1. Plants deficient for SMG7 exhibit growth defects and sterility. (A) Schematic representation of the *Arabidopsis SMG7* gene with the indicated T-DNA insertions in the *smg7-1*, *smg7-3* and *smg7-5* alleles (see supplementary material Fig. S2 for the molecular structure of the insertions). White boxes represent exons. (B) Northern blot hybridization analysis showing the expression of the *SMG7* gene in the indicated tissues. Full-length *SMG7* cDNA was used as a probe. RNA loading was monitored by hybridization with a probe specific for the *ACTIN2* (*ACT2*) gene. (C) Expression of the truncated transcripts from the *SMG7* loci in *smg7-1* and *smg7-3* mutants. A molecular-weight marker is indicated. (D-H) Vegetative-growth phenotypes. (D) A silique from a plant heterozygous for the *smg7-5* mutation with aborted seeds (indicated by arrowheads). (E) *smg7-1* mutant plant 4 weeks after germination. Scale bar: 0.5 cm. (F) *smg7-3* mutant plant germinated and grown for 4 weeks in soil. A control wild-type (wt) plant is indicated on the left. (G) 8-week-old *smg7-1* mutant, which was grown for 3 weeks on agar before being transferred to soil. A 4-week-old wild-type plant is shown on the left. (H) Inflorescence bolts from wild-type and *smg7-1* mutant plants. (I) Viable pollen grains in wild-type anthers have a dark-blue appearance after Alexander staining. Anthers of *smg7* mutants are usually empty or contain only a few nonviable pollen-like structures that stain green. Scale bars: 0.1 mm.

consequence of telomere dysfunction because neither chromosome end-to-end fusions nor telomere-length deregulation was detected in *smg7-1* mutants (data not shown).

Arabidopsis SMG7 is involved in NMD

Because the SMG7 protein was originally identified in a screen for components of the NMD pathway in *Caenorhabditis elegans* (Cali et al., 1999), we investigated whether *Arabidopsis* SMG7 contributes to NMD in plants, by monitoring the levels of alternatively spliced mRNA variants that bear a premature termination codon (PTC). The At5g62760 gene produces two alternatively spliced mRNAs, one of which contains a PTC (Fig. 2A) (Hori and Watanabe, 2005). The At5g62760 mRNA variants differ by 56 nucleotides and can be separated by agarose gel electrophoresis (Fig. 2B). Quantification of the RT-PCR products revealed that the abundance of the PTC-containing transcript was significantly increased relative to a spliced variant without a PTC in *smg7-1* mutants (P=0.0013; Fig. 2).

We further tested levels of two additional PTC-containing transcripts that are derived from the At2g45670 and At1g51340 loci and that are upregulated in NMD-deficient plants (Hori and Watanabe, 2005). Because alternatively spliced variants of the genes differ only by several nucleotides, we analyzed their relative abundance by directly sequencing products of the RT-PCR reactions that amplified regions spanning splicing junctions. Peaks derived from each splice variant could be distinguished on sequencing chromatograms and quantified. Using this technique, we detected a marginally significant increase of the At5g62760 PTC-containing transcript in *smg7-1* mutants (Table 1), which corroborated results obtained by Southern blot analysis (Fig. 2B). Levels of the PTC-containing At2g45670 and At1g51340 transcripts were significantly higher in *smg7-1* mutants than in wild-type plants (Table 1). These data show that SMG7 is important for the downregulation of PTC-containing mRNAs and strongly indicate that the SMG7 protein contributes to NMD in plants.

SMG7 is required for progression through meiotic anaphase II

To uncover the causes of sterility observed in *smg7* mutants, we analyzed male gametogenesis and sporogenesis. Closer inspection of anthers revealed that *smg7* plants fail to produce pollen and occasionally form structures that resemble aberrant non-viable pollen grains (Fig. 1I). This finding indicates that *SMG7* is required for initiation or progression of a developmental program that leads to the formation of male gametophytes. We further investigated the cause of sterility in *smg7* mutants by cytological examination of meiosis in pollen mother cells (PMCs). The first meiotic division in *smg7* mutants appeared to progress normally (Fig. 3J-M). We did not observe any abnormalities in homologous-chromosome pairing or synapsis during prophase I, as judged from three-dimensional fluorescence in situ hybridization (3D-FISH) and from immunolocalization of ASY1 (data not shown), a protein closely associated with the axial elements of the synaptonemal complex (Armstrong et al., 2002). Homologous chromosomes separated during anaphase I and formed two nuclei at the end of meiosis I (Fig. 3M). However, the second meiotic division was disrupted in *smg7* mutant plants. Although the SMG7-deficient plants entered meiosis II, the second meiotic division was not completed. We detected regular metaphase II (M2) and anaphase II (A2) meiocytes (Fig. 3N,O), but failed to detect any telophase II (T2) or tetrad stages. Instead, we frequently observed meiocytes that contained condensed separated chromatids that were irregularly localized within the cell (Fig. 3P,Q and Fig. 4A). In some meiocytes, the distribution of chromosomes appeared to reflect the position of the A2 spindle, forming two clearly distinguishable groups of chromatids (‘irregular A2’; Fig. 3P). In the remaining meiocytes, chromatids were randomly dispersed throughout the cell space (‘scattered chromatids’; Fig. 3Q). Chromosome-specific 3D-FISH confirmed a bilateral distribution of homologous chromatids in ‘irregular A2’ PMCs (Fig. 3V), whereas the position of the homologs in meiocytes at the ‘scattered chromatids’ stage was random (Fig. 3W). The occurrence of the two modes of chromatid distribution after M2 in

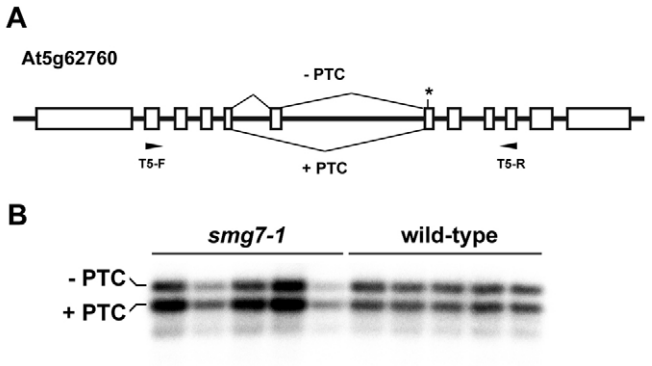

Fig. 2. SMG7 deficiency increases the level of a PTC-containing transcript. (A) Alternative splicing of the At5g62760 gene produces a transcript containing a premature termination codon (+PTC) in the seventh exon (indicated by an asterisk) (Hori and Watanabe, 2005). (B) Detection of the At5g62760 transcripts by RT-PCR and Southern blot analysis. The quantity of the –PTC and +PTC transcripts was determined by quantitative RT-PCR analysis using primers T5-F and T5-R (see Materials and Methods; indicated in A). The relative quantity of the transcripts was determined by the signal ratio of +PTC to –PTC for each sample. The average ratios for +PTC to –PTC for wild-type and *smg7-1* samples were 1.05±0.05 and 1.58±0.27, respectively.

Table 1. Ratio of –PTC to +PTC transcripts determined by direct sequencing of RT-PCR products

Locus	Wild type[a]	*smg7-1*	*P*[b]
At5g62760	1.92±0.53 (*n*=12) 1.42±0.41 (*n*=12)	4.05±0.99 (*n*=12) 2.77±0.82 (*n*=12) 2.98±0.88 (*n*=12)	0.061
At2g45670	0.29±0.13 (*n*=15) 0.37±0.17 (*n*=15) 0.26±0.15 (*n*=15)	1.99±0.74 (*n*=15) 1.53±0.94 (*n*=15)	0.004
At1g51340	0.26±0.13 (*n*=17) 0.24±0.13 (*n*=17) 0.21±0.11 (*n*=17)	0.49±0.24 (*n*=17) 0.42±0.21 (*n*=17)	0.006

RT-PCR products from two or three independent plants were quantified in each category. [a]Data are presented as the ratio of –PTC to +PTC transcript for each reaction ± s.d.; *n*, number of nucleotide positions that were quantified for each transcript. [b]*P* indicates significance of the difference between wild-type and *smg7-1* mutants. Statistic evaluation was performed with repeated measures ANOVA.

smg7 PMCs suggests that chromatids are first dispersed between opposite poles of the A2 spindles before drifting to random locations within the meiocyte.

We next investigated whether the abnormal chromosomal localization in *smg7* mutants is associated with an aberrant structure of the meiotic spindle. We did not detect any obvious irregularities in the structure of the spindle by tubulin immunodetection during the first meiotic division (supplementary material Fig. S3). During the second meiotic division, wild-type M2 chromosomes are attached to two short bipolar spindles (Fig. 5A), which start to stretch when chromatids separate during A2 (Fig. 5B,C). The resulting haploid nuclei are then mutually interconnected with dense arrays of microtubules that define boundaries for cytokinesis (Fig. 5D). Although a typical spindle can be detected in *smg7* mutants during M2 or early A2 (Fig. 5E), the later stages of meiosis displayed abnormalities in the arrangement of microtubules (Fig. 5F-H). Chromosomes in the meiocytes in the 'irregular A2' stage were aligned along spindles of abnormal shape and size (Fig. 5F), and multiple spindle-like structures were detected (Fig. 5G). At the 'scattered chromatids' stage, individual chromosomes were interconnected with bundles of microtubules (Fig. 5H). These data indicate that *smg7* deficiency impedes reassembly of the meiotic spindle during A2; this hindrance might contribute to the random distribution of chromatids at the end of meiosis II.

'Irregular A2' or 'scattered chromatids' meiocytes were among the most frequently detected meiotic stages in *smg7* anthers. Although chromosomes in *smg7* mutants eventually decondensed (Fig. 3R,S), forming PMCs with multiple micronuclei, cytokinesis was very rare (Fig. 3T). These data indicate that progression of meiosis in *smg7* plants is arrested or significantly delayed at the A2-T2 transition, when sister chromatids are separated but fail to decondense and to form nuclei. Progression of meiosis in wild-type *Arabidopsis* PMCs is highly synchronous with a slow prophase I followed by the first and second meiotic divisions that advance relatively quickly compared with prophase I (Armstrong et al., 2001). To assess progression of meiosis in *smg7* mutants, we examined the abundance of individual meiotic stages during flower development. The results of our staging experiment are consistent with the published data (Armstrong et al., 2001): only 18% of the meiocytes were between the M1 and T2 stages in wild-type floral buds that ranged from 0.3 to 0.4 mm (Fig. 4A). By contrast, 75% of PMCs in *smg7* buds at the corresponding developmental stage were at the A2-T2 transition. Cytokinesis in wild-type flowers was completed when buds reached 0.5 mm. However, the majority of meiocytes in *smg7* 0.4- to 0.5-mm buds still contained condensed chromatids and no cytokinesis could be detected in 0.5- to 0.7-mm floral buds (Fig. 4A). At this stage, wild-type anthers contained unicellular microspores coated with exine. The major component of exine is sporopollenin, which is secreted by the surrounding tapetum cells and forms a characteristic pattern on the surface of microspores (Scott et al., 2004) (Fig. 4B). Although cytokinesis was not completed in *smg7* mutants, tapetum cells still released sporopollenin, which was deposited on the surface of PMCs in the form of droplets (Fig. 4B). This further supports the notion that the development of germline cells in *smg7* mutants is arrested or significantly delayed relative to the surrounding sporophytic tapetum cells.

One of the hallmarks of the metaphase-telophase transition is a rapid dephosphorylation of histone H3. Immunolabeling of chromosomes with an antibody recognizing H3 Ser10 phosphorylation revealed that slow chromosome decondensation in *smg7* mutants is accompanied by delayed H3 Ser10 dephosphorylation (supplementary material Fig. S4). Although histone H3 phosphorylation diminishes during wild-type A2, it can still be readily detectable in a fraction of 'scattered chromatids' meiocytes, and even in some polyads in *smg7* mutants (supplementary material Fig. S4J-L).

Mutations in *Arabidopsis* meiotic genes often affect male and female meiosis differently (reviewed in Ma, 2005). To examine the effect of SMG7 deficiency on female fertility, we pollinated *smg7-1* flowers with wild-type pollen. Whereas the yield of seeds from control wild-type crosses was 25.3±9.0 per silique (*n*=12), *smg7-1* plants produced, on average, 1.7±1.9 seeds per silique (*n*=15), indicating that female fertility is significantly reduced, but not completely lost. Cytogenetic analysis of megaspore mother cells (MMCs) in *smg7-1* mutants revealed cells with separated and disorganized chromatids that resembled 'irregular A2' figures detected in PMCs (supplementary material Fig. S5). These data indicate that the *smg7-1* mutation has a similar effect on both male and female meiosis, but that the expressivity of the mutation appears to be lower in female meiosis.

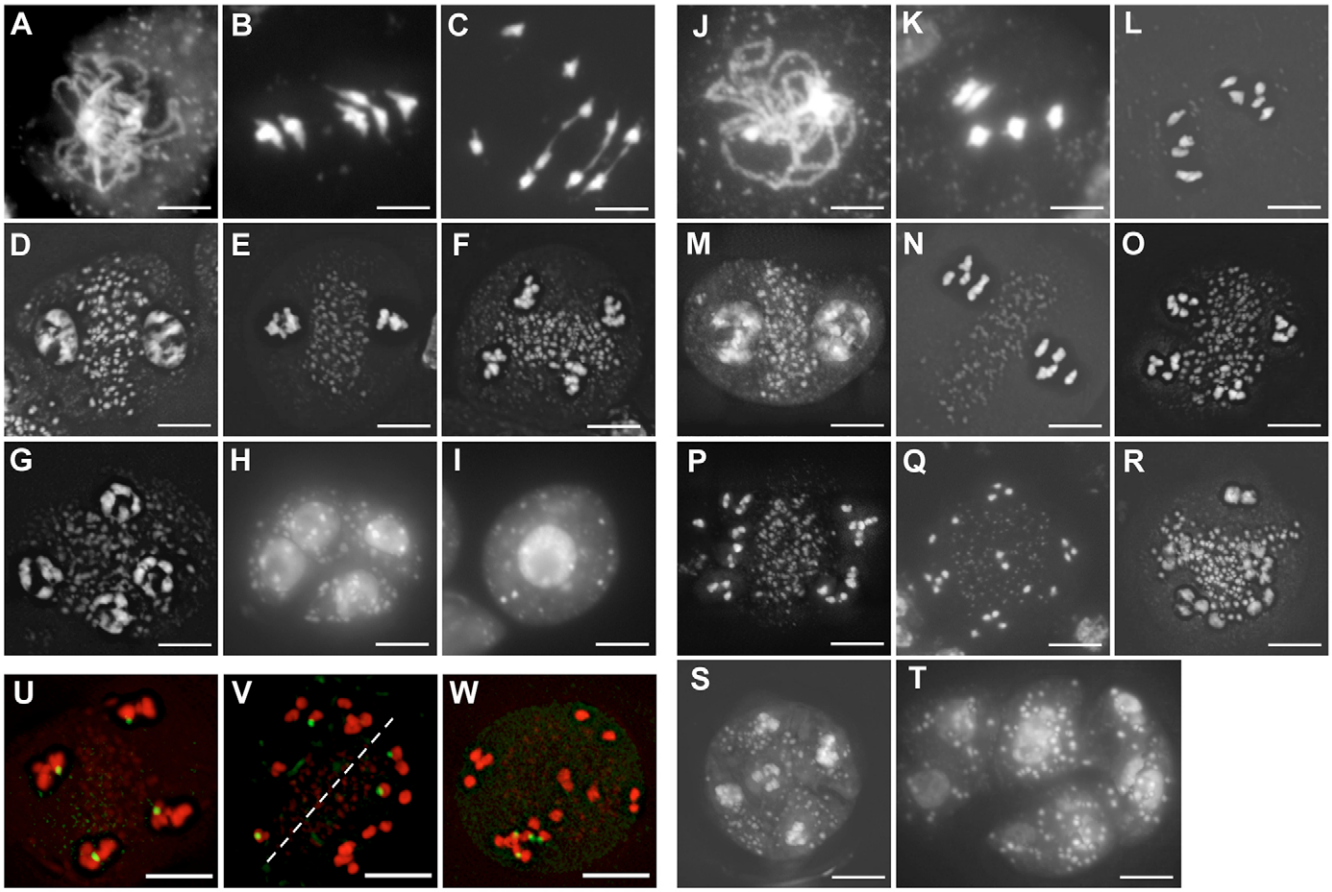

Fig. 3. Aberrant meiosis in SMG7-deficient PMCs. (A-I) Meiosis in wild-type PMCs. (J-T) Meiosis in *smg7-1* PMCs. (A,J) Pachytene, (B,K) metaphase I, (C,L) anaphase I, (D,M) telophase I, (E,N) metaphase II, (F,O) anaphase II. (G-I) Telophase II (G) in wild-type PMCs is followed by cytokinesis that results in the formation of tetrads (H) and microspores (I). (P,Q) *smg7* mutants fail to decondense chromosomes during the second meiotic division, resulting in 'irregular anaphase II' (P) and 'scattered chromatids' (Q) meiocytes. (R-T) Decondensed chromosomes tend to cluster (R,S), forming polyads (T). (U-W) The distribution of chromosome 4 during late meiosis II was investigated by 3D-FISH with a chromosome-4-specific probe (green) in wild-type (U) and *smg7-1* (V,W) plants. (U) Regular separation of chromosome 4 in A2. (V) Bilateral distribution of chromosome 4 during 'irregular A2'. The broken line separates the products of the first meiotic division. (W) The clustering of chromosome 4 in the 'scattered chromatids' meiocyte indicates random distribution of chromosomes at this stage. A-C and J-L were prepared by spreading PMCs fixed in ethanol:acetic acid (3:1; v/v) for better chromosome morphology. To preserve the 3D organization of the chromosomes in late meiotic PMCs (D-I, M-T and the 3D-FISH preparations U-W), cells were prepared from floral buds fixed in 4% paraformaldehyde. Scale bars: 5 μm.

The delayed chromosome decondensation, aberrant spindle reorganization and inefficient cytokinesis argue that the *Arabidopsis* SMG7 protein is required for progression from A2 to T2. The anaphase-telophase transition is characterized by an abrupt decrease in CDK activity and rapid dephosphorylation of CDK substrates. Our observations indicate that *Arabidopsis smg7-1* and *smg7-3* mutants might fail to efficiently downregulate CDK activity during the second meiotic division. Anaphase-like arrest has been induced in human cell lines by depleting Shugoshin (McGuinness et al., 2005), a kinetochore protein that prevents premature loss of centromeric cohesion during mitotic prophase. In this case, premature separation of sister chromatids during mitotic prophase prevents chromosome biorientation and, hence, inactivation of the spindle checkpoint.

To investigate whether the *smg7* phenotype arises from a failure to inactivate the spindle checkpoint owing to the premature separation of sister chromatids, we analyzed centromeric cohesion in meiotic interkinesis by FISH. Typically, five centromeric signals can be detected per interkinesis nucleus (Fig. 6B,C). Premature chromatid separation would result in split centromeric signals. We found only one separated centromere in 88 scored *smg7* interkinesis nuclei. We next studied whether meiotic chromosomes properly biorient at the M2 plate. Chromosome biorientation produces tension at sister kinetochores, which is a prerequisite for spindle-checkpoint inactivation. Chromosome biorientation in *Arabidopsis* M2 can be assessed from the morphology of the centromeric FISH signal, which is stretched owing to the tension produced by attachment of the sister kinetochores to the opposite spindle poles (Fig. 6E,F). All 150 chromosomes in 30 M2 plates that were analyzed in *smg7* mutants exhibited centromeric tension, indicating that chromosomes properly biorient. On the basis of these observations, we conclude that SMG7 deficiency does not cause premature separation of sister chromatids before biorientation. This indicates that the M2 spindle checkpoint is shut down in *smg7* mutants, thus activating the APC activator Cdc20 (APC^{Cdc20}) and allowing normal entry into A2.

It has been shown that expression of a non-degradable version of *Drosophila* cyclin B in mitotic cells leads to an anaphase arrest

with separated chromatids oscillating between the spindle poles (Parry and O'Farrell, 2001; Parry et al., 2003), which is reminiscent of the phenotype we observed in *smg7* meiosis. To determine whether aberrant proteolysis can induce similar A2 arrest, we treated *Arabidopsis* meiocytes with the 26S proteasome inhibitor MG115 (Planchais et al., 2000). We used the transpiration stream to deliver the inhibitor MG115 into intact flowers and cytologically analyzed meiocytes 4 hours after the application of the drug. We found 18 meiocytes that resembled 'scattered chromatids' stages of *smg7* mutants (Fig. 7) in three independent treatments (437 meiocytes were scored in total). Such meiocytes were never detected in control experiments without MG115 (520 meiocytes scored), demonstrating that inhibition of proteolysis can mimic the *smg7* phenotype.

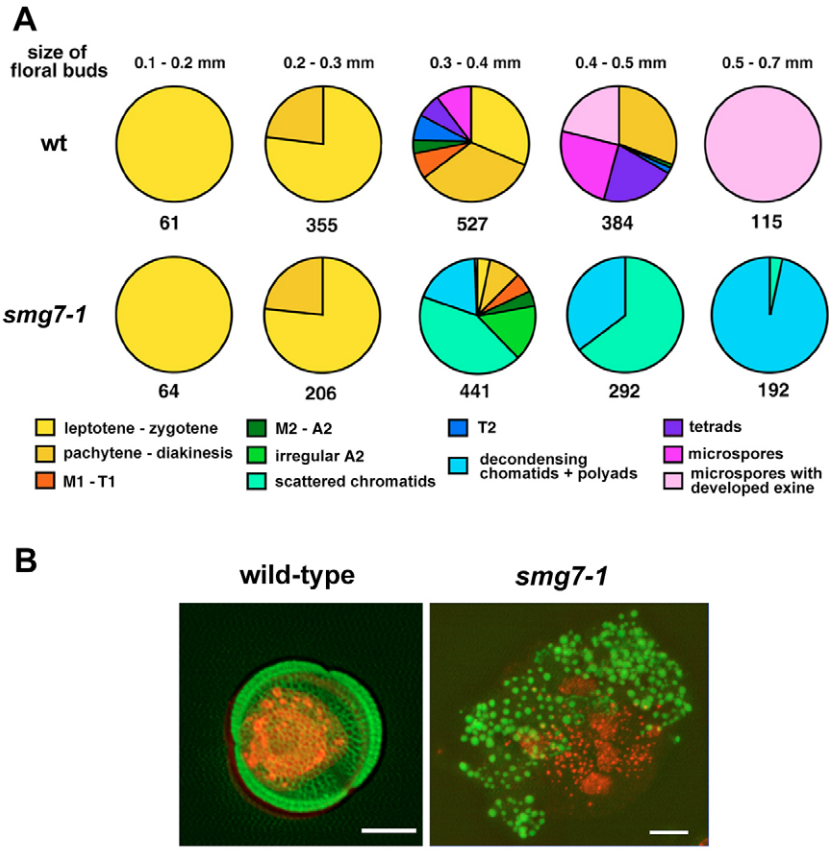

Fig. 4. The meiotic cell cycle is significantly delayed at the anaphase-II–telophase-II transition in *smg7* mutants. (A) Frequency of different stages of meiosis in developing floral buds. The total number of meiocytes is indicated below each pie chart. Nearly identical frequencies of prophase I stages in wild-type and *smg7-1* 0.1- to 0.3-mm buds demonstrate that progression of early meiosis correlates with flower development in *smg7* mutants. (B) Deposited sporopollenin (green) on the surface of wild-type mononuclear microspore and *smg7-1* polyad. DNA is counterstained with DAPI (red). Scale bars: 5 µm.

Discussion

SMG7-like proteins, which are characterized by EST1-TPR and EST1-CD domains, can be found in the majority of multicellular eukaryotes, including vertebrates, plants and insects. Our current understanding of the function of this evolutionarily conserved group of proteins in higher eukaryotes is mostly based on biochemical and functional studies in human cell lines. These data indicate that all three human paralogs (SMG5, SMG6 and SMG7) are involved in NMD (Ohnishi et al., 2003; Unterholzner and Izaurralde, 2004; Lee et al., 2006); additionally SMG5 and SMG6 also regulate telomere maintenance (Reichenbach et al., 2003; Snow et al., 2003). Together with a recent study demonstrating the involvement of the Est1-related Ebs1 protein in NMD in yeast (Luke et al., 2007), our data showing that SMG7 deficiency causes the upregulation of PTC-containing transcripts in *Arabidopsis* indicates that SMG7 (EST1)-like proteins are conserved components of the core NMD machinery.

In addition to the conserved function of SMG7 in the downregulation of aberrant mRNAs, we describe a novel role for the *Arabidopsis* SMG7 protein in regulation of the meiotic cell cycle. Hypomorphic non-lethal *smg7* alleles render *Arabidopsis* plants fully sterile owing to a failure in completing the anaphase-telophase transition in the second meiotic division. Anaphase arrest is very unusual because activation of separase, which triggers entry into anaphase, and destruction of M-type cyclins required for transition to telophase are coupled via activation of APC^{Cdc20} at the end of metaphase. One mechanism that could uncouple these two events is a premature loss of sister-chromatid cohesion before spindle-checkpoint inactivation. Such a mechanism has been described to cause an anaphase-like arrest in mitotic cells that were depleted of Shugoshin (Salic et al., 2004; Tang et al., 2004; Kitajima et al., 2005; McGuinness et al., 2005). However, our observation that centromeric cohesion is preserved in *smg7* mutants until all chromosomes biorient at the metaphase II plate argues that the spindle checkpoint is shut off and that *smg7* cells enter a regular anaphase II, suggesting that SMG7 acts downstream of APC^{Cdc20} activation.

The key mechanism that drives mitotic exit is the downregulation of CDK activity through proteasome-dependent degradation of M-type cyclins. *Drosophila* mutants deficient for the *cortex* gene, which encodes a germline-specific Cdc20 subunit of the APC, display a similar defect in chromosome decondensation and exit from meiosis as do *Arabidopsis smg7* mutants (Page and Orr-Weaver, 1996; Chu et al., 2001). The meiotic arrest of the *cortex* mutants appears to be caused by a defect in the degradation of cyclin A (Swan et al., 2005). It is well-established that the expression of a non-degradable version of cyclin B induces anaphase arrest in animal cells (Holloway et al., 1993; Parry and O'Farrell, 2001; Potapova et al., 2006; Wolf et al., 2006). Degradation of B-type cyclins also appears to be crucial for mitotic exit and cytokinesis in plants (Weingartner et al., 2004). Real-time imaging in fly and human mitotic cells shows that chromosomes that are halted at anaphase by expressing non-degradable cyclin B make oscillatory movements between the poles of the spindle (Parry and O'Farrell, 2001; Wolf et al., 2006). A similar phenomenon might be responsible for the arrangement of chromosomes in *smg7* mutants ('irregular A2'; Fig. 3P,Q). Recent studies have shown that the key players in anaphase chromosome decondensation and spindle stability are directly regulated by cyclin-B-dependent CDK activity (Vagnarelli et al., 2006; Woodbury and Morgan, 2007). Hence, the chromosome mislocalization, delayed chromatin decondensation and histone H3 dephosphorylation, and aberrant spindle rearrangements that are

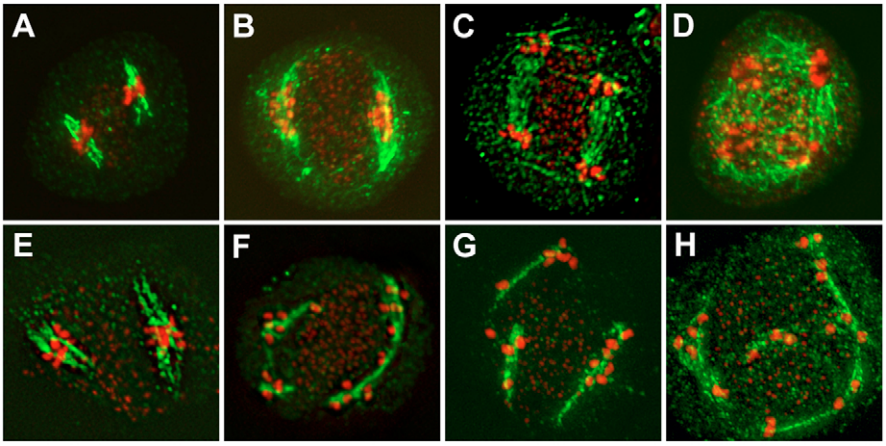

Fig. 5. Abnormal rearrangement of the spindle in late *smg7* meiosis. (A-D) Meiosis II spindle in wild-type PMCs. (A) M2, (B) early A2, (C) late A2, (D) T2. (E-H) Meiosis II spindle in *smg7-1* mutants (see Results for details).

observed in *smg7* mutants strongly indicate that SMG7 is important for the downregulation of cyclin-B-dependent CDK activity after chromosome separation in meiosis II. We tried to gain support for this scenario by studying the cellular localization of cyclin B1;1. However, we found that cyclin B1;1 is specific to mitotic cells and is not present in meiocytes (N.R. and K.R., unpublished data). The *Arabidopsis* genome encodes at least ten other cyclin-B-like molecules (Wang et al., 2004) and further studies are necessary to identify the cyclins important for meiosis.

SMG7 could regulate CDK activity by several mechanisms. The protein might facilitate proteolytic degradation of meiotic cyclins via the APC. Our ability to mimic anaphase II arrest by a chemical inhibitor of the 26S proteasome is consistent with this idea. Alternatively, SMG7 could regulate cyclin levels by affecting the stability of cyclin mRNA. Our data also indicate that *Arabidopsis* SMG7 contributes to NMD in plants. However, *Arabidopsis* plants deficient for the key NMD factors UPF1 and UPF3 are fertile and exhibit a set of phenotypes distinct from *smg7* mutants (Arciga-Reyes et al., 2006; Yoine et al., 2006) (R.A.I and D.E.S., unpublished data). Thus, inefficient NMD does not appear to be the major cause of the phenotypes observed in *smg7* mutants. A valuable hint as to the molecular mechanism underlying the function of the SMG7-like proteins was provided by an analysis of the crystal structure of human SMG7 (Fukuhara et al., 2005). This study revealed that the N-terminal EST1-TPR domain exhibits a fold that is similar to the 14-3-3-like proteins and features phosphoserine-binding activity. In the NMD pathway, human SMG5 and SMG7 proteins bind phosphorylated UPF1 and facilitate its dephosphorylation through protein phosphatase 2A (Ohnishi et al., 2003). *Arabidopsis* SMG7 might regulate cell-cycle progression in an analogous manner and antagonize CDK activity by mediating dephosphorylation of the CDK–cyclin-B substrates during anaphase.

Strikingly, the *smg7-1* and *smg7-3* mutants do not grossly affect mitotic progression, because we did not observe mitotic cells derived from floral tissues arrested at the anaphase-telophase transition (supplementary material Table S1). Although hypomorphic *smg7* mutants exhibit aberrant vegetative growth, this phenotype is modulated by environmental conditions, which makes it very unlikely to be a consequence of a fundamental mitotic defect. Rather, we postulate that the *Arabidopsis* SMG7 protein plays a pleiotropic role in several cellular processes. This is supported by the identification of a separation-of-function allele that causes infertility but does not impair vegetative growth and development (N.R. and K.R., unpublished data). Future analysis of this essential and evolutionarily conserved gene will probably uncover new regulatory pathways governing cell-cycle progression and responses to environmental stimuli.

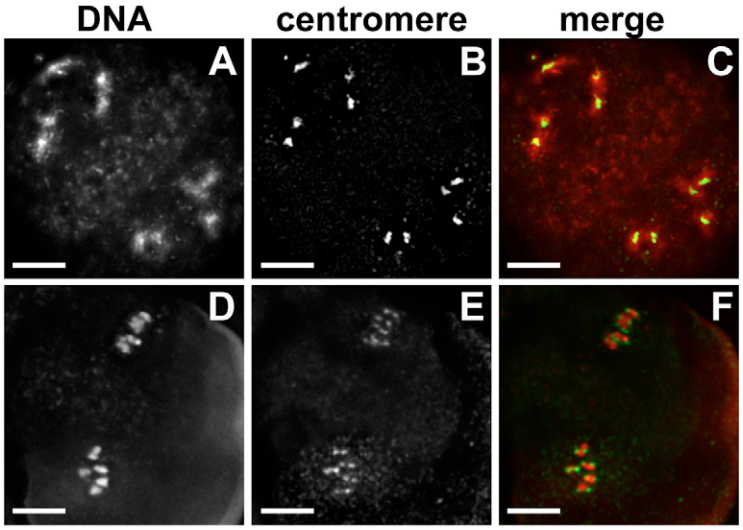

Fig. 6. Centromeric cohesion in meiotic interphase and metaphase II in *smg7-1* mutants. Centromeric DNA was analyzed by FISH with a 180-bp centromeric-repeat probe. (A-C) Representative examples of interkinesis; (D-F) M2. The centromeric probe was labeled with fluorescein (green) and DNA was counterstained with DAPI (red).

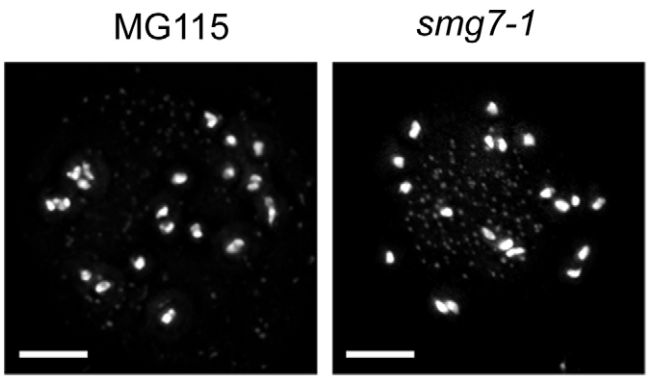

Fig. 7. MG115 treatment mimics the *smg7* phenotype. A wild-type PMC treated with the proteasome inhibitor MG115 contains randomly dispersed separated chromatids (left panel). Irregular A2 detected in a non-treated *smg7-1* mutant is shown at the right.

Materials and Methods

Plant growth conditions and treatments

Seeds of *Arabidopsis* plants were either directly sown on soil or germinated on MS medium supplemented with 1% (w/v) sucrose and 0.6% (w/v) plant agar (Ducheva, Netherlands). 3-week-old seedlings were transferred to soil. Plants were grown at 20-22°C at 40-45% humidity with a photoperiod of 16-hours of light to 8-hours of dark. *Arabidopsis* lines carrying *smg7-1*, *smg7-3* or *smg7-5* alleles were obtained from the Nottingham *Arabidopsis* Stock Centre (lines SALK_073354, SALK_112476 and SALK_144162, respectively) (Alonso et al., 2003). The inhibitor MG115 was applied by immersing cut stems bearing an inflorescence in a 500-μM solution of MG115 (Sigma, USA) in water. Floral buds were harvested for cytology 4 hours after MG115 application.

Molecular characterization of the *smg7-1* and *smg7-3* alleles

Plants heterozygous for the *smg7-1* allele were identified by PCR using primers LBc-1 (5′-TGGACCGCTTGCTGCAACTCT-3′), EST1b-1 (5′-GACCTTGGTAGCTG-GTCCTGAG-3′) and EST1b-2 (5′-GGACAACAGGCCAACCATTCAAC-3′). Plants carrying the *smg7-3* allele were genotyped from primers LBc-1, EST1b-13 (5′-GTGATTGGGCTGGCTGAGG-3′) and EST1b-14 (5′-CGCTTGGAC-CTACGTTTATTGATG-3′). To determine the structure of the borders of the insertions, the obtained PCR products were cloned into the pCR2.1-TOPO vector and sequenced.

RNA analysis

Total RNA was extracted using TriReagent solution (Sigma). For northern blot analysis, 10-μg aliquots were separated on a 1.2% formaldehyde agarose gel, blotted onto a nylon membrane and hybridized with a ^{32}P-labeled *SMG7* cDNA probe. RNA loading was checked by rehybridization with an *ACTIN2* probe (gene At5g0980). The quantity of the –PTC and +PTC transcripts was determined by RT-PCR. Approximately 2 μg of total RNA from flowers was subjected to reverse transcription using oligo dT. At5g62760 cDNA was amplified by 30 cycles of PCR with primers T5-F (5′-GCTACGAACCTGAGATGGAAG-3′) and T5-R (5′-TCCATGTC-CATATCCACCTCC-3′). The +PTC (362 bp) and –PTC (418 bp) PCR products were separated on 3% agarose gels, blotted onto a nylon membrane and hybridized with a ^{32}P-labeled At5g62760 gene fragment spanning the seventh to tenth exons. The membrane was exposed to a Kodak Phosphor Screen (BioRad) and scanned with Molecular Imager FX (BioRad). The autoradiogram was analyzed using QuantityOne software (BioRad). At2g45670 cDNA was amplified with primers NMD2-F (5′-CTCTTCTCTTTTGGCTATCAG-3′) and NMD2-R (5′-AAAGCACCGAGTTG-GAAGGAA-3′), and At1g51340 cDNA with primers NMD1-F (5′-TGTGTAACTCTCTCCGCGTC-3′) and NMD1-R (5-TGCCACAAACG-GAAGTCCTA-3′). Amplified RT-PCR products were sequenced using a BigDye terminator and ABI310 sequencer (Applied Biosystems, CA). Sequencing reactions were quantified as described previously (Hori and Watanabe, 2005). Three independent RNA samples were analyzed from each wild type and *smg7-1* mutant, and at least 12 independent nucleotide positions were quantified for each transcript. Statistical evaluation was performed using repeated measures analysis of variance.

Cytology and immunofluorescence microscopy

Meiotic spreads were obtained from anthers as described previously (Puizina et al., 2004). For analysis of chromosome distribution in meiocytes, floral buds were fixed in 4% (w/v) paraformaldehyde in PBS buffer. Floral tissues were macerated in 2.5% cellulase (w/v; Onozuka R-10, Serva), 2.5% pectolyase (w/v; Sigma), 2.5% pectinase (w/v; Sigma) and 0.5% cytohelicase (w/v; Sigma) in PBS buffer for 30 minutes at 37°C. Dissected anthers were gently squashed on poly-L-lysine-coated slides and meiocytes were subjected to FISH or stained with 4′,6-diamidino-2-phenylindole (DAPI) (2 μg/ml). FISH was performed as described (Siroky et al., 2003) using a 180-bp *Arabidopsis* centromeric repeat or BAC clones T22F8 and T5J17 (*Arabidopsis* Biological Resource Centre, OH) derived from the right arm of *Arabidopsis* chromosome 4 as probes. Spindle structure was visualized using a rat anti-α-tubulin antibody (dilution 1:25; Serotec) and a Cy3-conjugated anti-rat IgG antibody according to Peirson et al. (Peirson et al., 1997). Histone H3 phosphorylation was detected as described (Manzanero et al., 2000) using rabbit antiserum specifically recognizing the histone H3 Ser10 phospho-epitope (Upstate Biotechnology, USA) and a Cy3-conjugated anti-rabbit IgG antibody. Meiocytes stained with DAPI or subjected to FISH or immunofluorescence were examined by 3D epifluorescence microscopy using a Zeiss Axioscope fluorescence microscope (Zeiss, Germany) equipped with a cooled CCD camera (Visitron, Germany). Optical sections (0.1 μm) were acquired using MetaVue software (Universal Imaging Corporation, USA) and processed by AutoDeblur deconvolution software (AutoQaunt, USA). Alexander staining for pollen viability was performed as described (Alexander, 1969).

We thank Lea Harrington for help with identifying *Arabidopsis* SMG7 homologs, and Maria Siomos, Jan-Michael Peters and Franz Klein for helpful discussion. We are also indebted to Chris Franklin for providing the anti-ASY1 antibody. This work was supported by the Austrian Science Fund (grant P19256-B03 to K.R.), NSF (MCB-0235987 to D.E.S.) and the Czech Science Foundation (522/06/0380 to J.S.).

References

Alexander, M. P. (1969). Differential staining of aborted and nonaborted pollen. *Stain Technol.* **44**, 117-122.

Alonso, J. M., Stepanova, A. N., Leisse, T. J., Kim, C. J., Chen, H., Shinn, P., Stevenson, D. K., Zimmerman, J., Barajas, P., Cheuk, R. et al. (2003). Genome-wide insertional mutagenesis of Arabidopsis thaliana. *Science* **301**, 653-657.

Altschul, S. F. and Koonin, E. V. (1998). Iterated profile searches with PSI-BLAST-a tool for discovery in protein databases. *Trends Biochem. Sci.* **23**, 444-447.

Arciga-Reyes, L., Wootton, L., Kieffer, M. and Davies, B. (2006). UPF1 is required for nonsense-mediated mRNA decay (NMD) and RNAi in Arabidopsis. *Plant J.* **47**, 480-489.

Armstrong, S. J., Franklin, F. C. and Jones, G. H. (2001). Nucleolus-associated telomere clustering and pairing precede meiotic chromosome synapsis in Arabidopsis thaliana. *J. Cell Sci.* **114**, 4207-4217.

Armstrong, S. J., Caryl, A. P., Jones, G. H. and Franklin, F. C. (2002). Asy1, a protein required for meiotic chromosome synapsis, localizes to axis-associated chromatin in Arabidopsis and Brassica. *J. Cell Sci.* **115**, 3645-3655.

Beernink, H. T., Miller, K., Deshpande, A., Bucher, P. and Cooper, J. P. (2003). Telomere maintenance in fission yeast requires an est1 ortholog. *Curr. Biol.* **13**, 575-580.

Borgne, A., Murakami, H., Ayte, J. and Nurse, P. (2002). The G1/S cyclin Cig2p during meiosis in fission yeast. *Mol. Biol. Cell* **13**, 2080-2090.

Cali, B. M., Kuchma, S. L., Latham, J. and Anderson, P. (1999). smg-7 is required for mRNA surveillance in Caenorhabditis elegans. *Genetics* **151**, 605-616.

Chiu, S. Y., Serin, G., Ohara, O. and Maquat, L. E. (2003). Characterization of human Smg5/7a: a protein with similarities to Caenorhabditis elegans SMG5 and SMG7 that functions in the dephosphorylation of Upf1. *RNA* **9**, 77-87.

Chu, T., Henrion, G., Haegeli, V. and Strickland, S. (2001). Cortex, a Drosophila gene required to complete oocyte meiosis, is a member of the Cdc20/fizzy protein family. *Genesis* **29**, 141-152.

de Gramont, A. and Cohen-Fix, O. (2005). The many phases of anaphase. *Trends Biochem. Sci.* **30**, 559-568.

Do, C. B., Mahabhashyam, M. S., Brudno, M. and Batzoglou, S. (2005). ProbCons: probabilistic consistency-based multiple sequence alignment. *Genome Res.* **15**, 330-340.

Fukuhara, N., Ebert, J., Unterholzner, L., Lindner, D., Izaurralde, E. and Conti, E. (2005). SMG7 is a 14-3-3-like adaptor in the nonsense-mediated mRNA decay pathway. *Mol. Cell* **17**, 537-547.

Galtier, N., Gouy, M. and Gautier, C. (1996). SEAVIEW and PHYLO_WIN: two graphic tools for sequence alignment and molecular phylogeny. *Comput. Appl. Biosci.* **12**, 543-548.

Gross, S. D., Schwab, M. S., Taieb, F. E., Lewellyn, A. L., Qian, Y. W. and Maller, J. L. (2000). The critical role of the MAP kinase pathway in meiosis II in Xenopus oocytes is mediated by p90(Rsk). *Curr. Biol.* **10**, 430-438.

Hall, T. A. (1999). BioEdit: a user-friendly biological sequence alignment editor and analysis program for Windows 95/98/NT. *Nucl. Acids Sym. Ser.* **41**, 95-98.

Hochegger, H., Klotzbucher, A., Kirk, J., Howell, M., le Guellec, K., Fletcher, K., Duncan, T., Sohail, M. and Hunt, T. (2001). New B-type cyclin synthesis is required between meiosis I and II during Xenopus oocyte maturation. *Development* **128**, 3795-3807.

Holloway, S. L., Glotzer, M., King, R. W. and Murray, A. W. (1993). Anaphase is initiated by proteolysis rather than by the inactivation of maturation-promoting factor. *Cell* **73**, 1393-1402.

Hori, K. and Watanabe, Y. (2005). UPF3 suppresses aberrant spliced mRNA in Arabidopsis. *Plant J.* **43**, 530-540.

Irniger, S. (2006). Preventing fatal destruction: inhibitors of the anaphase-promoting complex in meiosis. *Cell Cycle* **5**, 405-415.

Iwabuchi, M., Ohsumi, K., Yamamoto, T. M., Sawada, W. and Kishimoto, T. (2000). Residual Cdc2 activity remaining at meiosis I exit is essential for meiotic M-M transition in Xenopus oocyte extracts. *EMBO J.* **19**, 4513-4523.

Izawa, D., Goto, M., Yamashita, A., Yamano, H. and Yamamoto, M. (2005). Fission yeast Mes1p ensures the onset of meiosis II by blocking degradation of cyclin Cdc13p. *Nature* **434**, 529-533.

Kitajima, T. S., Hauf, S., Ohsugi, M., Yamamoto, T. and Watanabe, Y. (2005). Human Bub1 defines the persistent cohesion site along the mitotic chromosome by affecting Shugoshin localization. *Curr. Biol.* **15**, 353-359.

Lee, H., Sengupta, N., Villagra, A., Rezai-Zadeh, N. and Seto, E. (2006). Histone deacetylase 8 safeguards the human ever-shorter telomeres 1B (hEST1B) protein from ubiquitin-mediated degradation. *Mol. Cell. Biol.* **26**, 5259-5269.

Luke, B., Azzalin, C. M., Hug, N., Deplazes, A., Peter, M. and Lingner, J. (2007). Saccharomyces cerevisiae Ebs1p is a putative ortholog of human Smg7 and promotes nonsense-mediated mRNA decay. *Nucleic Acids Res*. **35**, 7688-7697.

Lundblad, V. (2003). Telomere replication: an Est fest. *Curr. Biol.* **13**, R439-R441.

Lundblad, V. and Szostak, J. W. (1989). A mutant with a defect in telomere elongation leads to senescence in yeast. *Cell* **57**, 633-643.

Ma, H. (2005). Molecular genetic analyses of microsporogenesis and microgametogenesis in flowering plants. *Annu. Rev. Plant Biol.* **56**, 393-434.

Manzanero, S., Arana, P., Puertas, M. J. and Houben, A. (2000). The chromosomal distribution of phosphorylated histone H3 differs between plants and animals at meiosis. *Chromosoma* **109**, 308-317.

Marston, A. L. and Amon, A. (2004). Meiosis: cell-cycle controls shuffle and deal. *Nat. Rev. Mol. Cell Biol.* **5**, 983-997.

McGuinness, B. E., Hirota, T., Kudo, N. R., Peters, J. M. and Nasmyth, K. (2005). Shugoshin prevents dissociation of cohesin from centromeres during mitosis in vertebrate cells. *PLoS Biol.* **3**, e86.

Ohnishi, T., Yamashita, A., Kashima, I., Schell, T., Anders, K. R., Grimson, A., Hachiya, T., Hentze, M. W., Anderson, P. and Ohno, S. (2003). Phosphorylation of hUPF1 induces formation of mRNA surveillance complexes containing hSMG-5 and hSMG-7. *Mol. Cell* **12**, 1187-1200.

Page, A. W. and Orr-Weaver, T. L. (1996). The Drosophila genes grauzone and cortex are necessary for proper female meiosis. *J. Cell Sci.* **109**, 1707-1715.

Page, S. L. and Hawley, R. S. (2003). Chromosome choreography: the meiotic ballet. *Science* **301**, 785-789.

Parry, D. H. and O'Farrell, P. H. (2001). The schedule of destruction of three mitotic cyclins can dictate the timing of events during exit from mitosis. *Curr. Biol.* **11**, 671-683.

Parry, D. H., Hickson, G. R. and O'Farrell, P. H. (2003). Cyclin B destruction triggers changes in kinetochore behavior essential for successful anaphase. *Curr. Biol.* **13**, 647-653.

Peirson, B. N., Bowling, S. E. and Makaroff, C. A. (1997). A defect in synapsis causes male sterility in a T-DNA-tagged Arabidopsis thaliana mutant. *Plant J.* **11**, 659-669.

Peters, J. M. (2006). The anaphase promoting complex/cyclosome: a machine designed to destroy. *Nat. Rev. Mol. Cell Biol.* **7**, 644-656.

Petronczki, M., Siomos, M. F. and Nasmyth, K. (2003). Un menage a quatre: the molecular biology of chromosome segregation in meiosis. *Cell* **112**, 423-440.

Planchais, S., Glab, N., Inze, D. and Bergounioux, C. (2000). Chemical inhibitors: a tool for plant cell cycle studies. *FEBS Lett.* **476**, 78-83.

Potapova, T. A., Daum, J. R., Pittman, B. D., Hudson, J. R., Jones, T. N., Satinover, D. L., Stukenberg, P. T. and Gorbsky, G. J. (2006). The reversibility of mitotic exit in vertebrate cells. *Nature* **440**, 954-958.

Puizina, J., Siroky, J., Mokros, P., Schweizer, D. and Riha, K. (2004). Mre11 deficiency in Arabidopsis is associated with chromosomal instability in somatic cells and Spo11-dependent genome fragmentation during meiosis. *Plant Cell* **16**, 1968-1978.

Queralt, E., Lehane, C., Novak, B. and Uhlmann, F. (2006). Downregulation of PP2A(Cdc55) phosphatase by separase initiates mitotic exit in budding yeast. *Cell* **125**, 719-732.

Reichenbach, P., Hoss, M., Azzalin, C. M., Nabholz, M., Bucher, P. and Lingner, J. (2003). A human homolog of yeast est1 associates with telomerase and uncaps chromosome ends when overexpressed. *Curr. Biol.* **13**, 568-574.

Salic, A., Waters, J. C. and Mitchison, T. J. (2004). Vertebrate shugoshin links sister centromere cohesion and kinetochore microtubule stability in mitosis. *Cell* **118**, 567-578.

Scott, R. J., Spielman, M. and Dickinson, H. G. (2004). Stamen structure and function. *Plant Cell* **16**, S46-S60.

Siroky, J., Zluvova, J., Riha, K., Shippen, D. E. and Vyskot, B. (2003). Rearrangements of ribosomal DNA clusters in late generation telomerase-deficient Arabidopsis. *Chromosoma* **112**, 116-123.

Snow, B. E., Erdmann, N., Cruickshank, J., Goldman, H., Gill, R. M., Robinson, M. O. and Harrington, L. (2003). Functional conservation of the telomerase protein Est1p in humans. *Curr. Biol.* **13**, 698-704.

Stegmeier, F. and Amon, A. (2004). Closing mitosis: the functions of the Cdc14 phosphatase and its regulation. *Annu. Rev. Genet.* **38**, 203-232.

Swan, A., Barcelo, G. and Schupbach, T. (2005). Drosophila Cks30A interacts with Cdk1 to target Cyclin A for destruction in the female germline. *Development* **132**, 3669-3678.

Tang, Z., Sun, Y., Harley, S. E., Zou, H. and Yu, H. (2004). Human Bub1 protects centromeric sister-chromatid cohesion through Shugoshin during mitosis. *Proc. Natl. Acad. Sci. USA* **101**, 18012-18017.

Taylor, S. S., Scott, M. I. and Holland, A. J. (2004). The spindle checkpoint: a quality control mechanism which ensures accurate chromosome segregation. *Chromosome Res.* **12**, 599-616.

Unterholzner, L. and Izaurralde, E. (2004). SMG7 acts as a molecular link between mRNA surveillance and mRNA decay. *Mol. Cell* **16**, 587-596.

Vagnarelli, P., Hudson, D. F., Ribeiro, S. A., Trinkle-Mulcahy, L., Spence, J. M., Lai, F., Farr, C. J., Lamond, A. I. and Earnshaw, W. C. (2006). Condensin and Repo-Man-PP1 co-operate in the regulation of chromosome architecture during mitosis. *Nat. Cell Biol.* **8**, 1133-1142.

Wang, G., Kong, H., Sun, Y., Zhang, X., Zhang, W., Altman, N., DePamphilis, C. W. and Ma, H. (2004). Genome-wide analysis of the cyclin family in Arabidopsis and comparative phylogenetic analysis of plant cyclin-like proteins. *Plant Physiol.* **135**, 1084-1099.

Watanabe, Y. (2004). Modifying sister chromatid cohesion for meiosis. *J. Cell Sci.* **117**, 4017-4023.

Weingartner, M., Criqui, M. C., Meszaros, T., Binarova, P., Schmit, A. C., Helfer, A., Derevier, A., Erhardt, M., Bogre, L. and Genschik, P. (2004). Expression of a nondegradable cyclin B1 affects plant development and leads to endomitosis by inhibiting the formation of a phragmoplast. *Plant Cell* **16**, 643-657.

Wolf, F., Wandke, C., Isenberg, N. and Geley, S. (2006). Dose-dependent effects of stable cyclin B1 on progression through mitosis in human cells. *EMBO J.* **25**, 2802-2813.

Woodbury, E. L. and Morgan, D. O. (2007). Cdk and APC activities limit the spindle-stabilizing function of Fin1 to anaphase. *Nat. Cell Biol.* **9**, 106-112.

Yoine, M., Ohto, M. A., Onai, K., Mita, S. and Nakamura, K. (2006). The lba1 mutation of UPF1 RNA helicase involved in nonsense-mediated mRNA decay causes pleiotropic phenotypic changes and altered sugar signalling in Arabidopsis. *Plant J.* **47**, 49-62.